Contents lists available at ScienceDirect

Chemical Engineering Research and Design

journal homepage: www.elsevier.com/locate/cherd

# A seven lumped kinetic model for industrial catalyst in DMTO process

Lei Ying[a,b], Xiaoshuai Yuan[b,c], Mao Ye[b,*], Youwei Cheng[a], Xi Li[a], Zhongmin Liu[b]

[a] Department of Chemical and Biochemical Engineering, Zhejiang University, Hangzhou 310027, China
[b] Dalian National Laboratory for Clean Energy and National Engineering Laboratory for MTO, Dalian Institute of Chemical Physics, Chinese Academy of Sciences, Dalian 116023, China
[c] University of Chinese Academy of Sciences, Beijing 100049, China

ARTICLE INFO

*Article history:*
Received 1 November 2014
Received in revised form 4 May 2015
Accepted 18 May 2015
Available online 27 May 2015

*Keywords:*
Methanol to olefins
Industrial catalyst
Kinetic model

ABSTRACT

Methanol to olefins (MTO) represents an important process for ethylene and propylene production from abundant natural materials, e.g. natural gas or biomass. This paper reports a lumped kinetic model for the MTO process over an industrial MTO catalyst, i.e. DMTO catalyst. The kinetic model takes into account seven lumps, i.e. methane, ethylene, propylene, propane, $C_4$, $C_5^+$ (including $C_5$, $C_6$ hydrocarbons and ethane) and coke. And a selective deactivation model was proposed to quantify the product selectivity and abrupt activity change in the MTO process. The kinetics under temperatures of 450 °C, 475 °C, and 490 °C, water/methanol mole ratio in the feed of 0, 2 and 4, and weight hour space velocity (WHSV) between 30 and 955 $g_{MeOH}\ g_{cat}^{-1}\ h^{-1}$ was studied. Experiments with small WHSV of 2.1 and 2.8 $g_{MeOH}\ g_{cat}^{-1}\ h^{-1}$ were further carried out to study the catalyst deactivation. The kinetic parameters were calculated by use of a nonlinear least square method, with special attention to the coke distribution along the axial distance. The proposed kinetic model is able to predict the product concentrations measured in the fixed bed reactor reasonable well, with relative deviations less than 5% for major species such as ethylene, propylene, butylenes and methanol.


## 1. Introduction

Light olefins (ethylene and propylene) are among the most demanded compounds in the petrochemical industry. They are conventionally produced by thermal cracking of naphtha and fluid catalytic cracking, which account for nearly 90 wt% of the world's olefins production (Aitani et al., 2000; Cavani and Trifiro, 1995; Chang et al., 1977; Jiang et al., 2008). In recent years, considerable efforts have been devoted to developing new processes for light olefins production because of the global shortage in oil reserves. Methanol to olefins (MTO) appears to be a promising way in this regard since methanol can be readily obtained from abundantly available resources such as natural gas, coal and biomass (Keil, 1999; Stocker, 1999).

The Dalian Institute of Chemical Physics (DICP), Chinese Academy of Sciences, has been involving in the MTO process development since 1980s (Liang et al., 1990). In 2010, the world's first commercial plant based on the DICP's MTO (DMTO) technology was successfully started up in North China (Zhao et al., 2013; Tian et al., 2015). The operation data shows that the maximum selectivity towards ethylene and propylene exceeds 80 wt% at full load (1.8 Mt/a MeOH feed). Although MTO process was industrialized, the kinetic model for industrial MTO catalyst, which is important for designing reactor and optimizing unit operation, still remains blank.

In the open literature there exists mainly two different types of kinetic models that have been developed for the MTO process, i.e., the detailed models (Mihail et al., 1983; Park and Froment, 2001a,b) and lumped models (Bos et al., 1995;

* *Corresponding author*. Tel.: +86 411 84379618; fax: +86 411 84379289.
E-mail address: maoye@dicp.ac.cn (M. Ye).
http://dx.doi.org/10.1016/j.cherd.2015.05.024

**Nomenclature**

| | |
|---|---|
| $A$, $B$, $D$ | constants |
| $C_C$ | weight percent of coke on the catalyst (g 100 $g_{cat}^{-1}$) |
| $C_0$ | initial concentration (mol $L^{-1}$) |
| $F_{MeOH}$ | mass flow rate of methanol (g $h^{-1}$) |
| $k_i$ | kinetic constant of step $i$ in the kinetic scheme (L $g_{cat}^{-1}$ $min^{-1}$) |
| $k_t$ | total rate constant of methanol ($g_{MeOH}$ $g_{cat}^{-1}$ $h^{-1}$) |
| $m$ | catalyst mass (g) |
| $Mw$ | molecular weight (g $mol^{-1}$) |
| $r_i$ | reaction rate for lump $i$ (mol $g_{cat}^{-1}$ $min^{-1}$) |
| $t$ | time (min) |
| $T$ | temperature (K) |
| $\upsilon_i$ | stoichiometric number |
| WHSV | weight hour space velocity ($g_{MeOH}$ $g_{cat}^{-1}$ $h^{-1}$) |
| $X$ | methanol conversion |
| $X_i$ | weight fraction of lump $i$ on a total basis |
| $X_W$ | water content in the feed |
| $z$ | dimensionless reactor length |
| $\alpha_i$ | empirical deactivation constant |
| $\varphi_i$ | deactivation function for component $i$ |

Chang, 1980; Chen et al., 2007; Fatourehchi et al., 2011; Gayubo et al., 2000; Kaarsholm et al., 2010; Menges and Kraushaar-Czarnetzki, 2012; Schoenfelder et al., 1994; Sedran et al., 1990a,b; Taheri Najafabadi et al., 2012). Mihail et al. (1983) reported a detailed model containing 53 reactions, while Park and Froment (2001a,b) developed a single event model at the elementary reaction level for the MTO process over HZSM-5 catalyst. Although the detailed models give a deep insight into the information of individual compounds, the lack of experimental information on the reaction intermediates may result in a poor prediction of the kinetic parameters. Furthermore, mathematical models of reactors incorporated with detailed kinetic model will bring about calculation difficulty. On the other hand, lumped models have been shown successful to a certain extend in the modeling of MTO reactors. Bos et al. (1995) performed kinetic experiments in a pulse-flow fixed bed reactor with pre-coked catalyst, and a model consists of 12 reactions has been proposed. Based on this lumped model, the authors studied various types of fluidized bed reactors with the conclusion that fast fluidized bed reactor and turbulent fluidized bed reactor would be the most suitable reactor configurations for the MTO process. Gayubo et al. (2000) proposed a five lumped kinetic model for methanol reaction over SAPO-34 catalyst, in which the influence of water on catalyst activity and selectivity has been considered. But this model requires a separate deactivation model when used for reactor design. Taheri Najafabadi et al. (2012) developed a kinetic model by considering the reaction mechanism based on data obtained by Alwahabi and Froment (2004). However the model was also limited to fresh catalyst. Obviously, all of the aforementioned kinetic models are established on laboratory synthesized SAPO-34 catalyst. It is argued that the performance of the SAPO-34 catalyst depends on the crystal sizes and acid strength (Alvaro-Munoz et al., 2012; Bleken et al., 2009; Haw, 2002; Yang et al., 2013), which are closely related to the synthetic procedures. Besides the excellent reaction performance, the industrial catalyst used in MTO process needs to maintain sufficient mechanical strength in order to minimize the catalyst attrition in the fluidized bed reactor. Therefore different synthetic procedures are followed in the production of the industrial MTO catalyst. Thus the reaction performance may differ significantly from that of laboratory synthesized SAPO-34 catalyst. Recently, Ying et al. (2013) established a simple five-lumped kinetic model for DMTO catalyst. In their work, the kinetic constants were calculated based on a dynamic two phase fluidized-bed model. The validity of the kinetics model, however, depends on the empirical hydrodynamics.

Methanol reaction over SAPO-34 catalyst is accompanied by a rapid deactivation due to the deposition of coke (referred to carbonaceous compounds) on the catalyst (Guisnet, 2002; Mores et al., 2008; Qi et al., 2007; Wei et al., 2012). Therefore a deactivation model, being able to predict the product selectivity dependence with coke content, is of great importance for the MTO process. Sedran et al. (1990a) found that the catalyst deactivation can be expressed as an exponential activity decay function, and the catalyst activity was directly related to the total hydrocarbon formed in the reactions. Bos et al. (1995) tested different empirical deactivation correlations proposed by Froment et al. (2010). The exponential correlation was found to best represent the effect of coke on the deactivation rate constants. Bilbao and his co-workers (Benito et al., 1996; Gayubo et al., 2007, 1996) performed extensive MTO experiments for different types of catalysts, and the authors concluded that the catalyst deactivation should be correlated with the composition of lumped species (i.e. oxygenates, light olefins, and the rest of the products). An oscillating microbalance reactor (TEOM) provides an opportunity for the instantaneous measurement of coke content during MTO reaction. Based on the experimental results collected from TEOM, Chen et al. (2007) found that a linear dependency between the coke content and the reaction rate gave the best representation of the experimental data. Generally, in most of the deactivation models reported for the MTO process, a single parameter, i.e. average coke content, was used to account for the effect of coke on catalyst activity and product selectivity. Actually in the fixed bed reactor, there exists a distribution of coke along the catalyst bed because of the lack of catalyst mobility (Kaarsholm et al., 2007). Consequently, the measured coke content from fixed bed experiments is always an average one, the value of which is obtained by homogenizing the coked and fresh catalyst. This treatment cannot reflect the essence of coke distribution on the deactivation and product selectivity.

In this work, a seven lumped kinetic model was developed based on the fixed bed kinetic experiments over SAPO-34 catalyst. Special attention was paid to coke distribution along the catalyst bed. The catalyst coke content was calculated simultaneously with the gas phase product distribution for different times on stream at different spatial positions. A selective deactivation model was proposed to account for the coke content on the catalyst activity and product selectivity.

## 2. Experimental

### 2.1. *Fixed bed reactor*

In all the kinetic experiments performed, an industrial MTO catalyst was used. The detailed characterization of the MTO catalyst are not shown in this paper because of commercial

**Table 1 – Properties of the catalyst.**

| Property | Value |
|---|---|
| Catalyst brand | DMTO catalyst |
| Catalyst manufacturer | Chia Tai Energy Materials Ltd. |
| Mean particle size (μm) | 82.3 |
| BET surface area ($m^2\ g^{-1}$) | 263.55 |
| Particle density ($kg\ m^{-3}$) | 1220 |

confidentiality, thus only some related properties of the catalyst that affect the reaction performance are given out in Table 1.

The catalyst was pressed and sieved to particle size of 40–60 mesh. Kinetic experiments were carried out at atmospheric pressure in a quartz glass tubular reactor of 4 mm internal diameter. Weight hourly space velocity (WHSV) was altered by loading different amount of catalyst while keeping the same methanol flow rate. Before each experimental run, the catalyst was heated to 500 °C and maintained for 1 h in nitrogen flow, and then the temperature was adjusted to the desired reaction temperature. Aqueous methanol solution fed by a piston pump passed through a vaporizer and then entered into the reactor. All the effluent products were kept warm and analyzed on line by use of Agilent 7890A gas chromatography equipped with a FID detector and a PoraPLOT Q-HT capillary column (25 m × 0.53 mm × 0.02 mm).

### 2.2. *Fluidized bed reactor*

Due to the inhomogeneous distribution of coke along the fixed bed, the deactivation characteristic of MTO reaction was studied in a batch fluidized bed reactor. Detailed operation of the fluidized bed has been described in the literature (Ying et al., 2013). For short, the fluidized bed reactor has an inner diameter of 0.019 m and a height of 0.35 m connected at the top to a filter to prevent entrainment of solid particles. The analysis of gaseous components is same as fixed bed operation. After a predefined times on stream, the catalyst was discharged and the coke content of the deactivated catalyst was measured by thermogravimetric analysis.

### 2.3. *Experimental results*

The MTO reaction is theoretically complex; abundant knowledge in regard to this reaction has been obtained through extensive experiments (Keil, 1999; Stocker, 1999). Typically, the distribution of reaction products reaches from $C_1$–$C_6$ hydrocarbons, with minor content in $C_6$ hydrocarbon because of product shape selectivity (Hereijgers et al., 2009). The reaction is influenced by various parameters, of which reaction temperature, water content and coke content may play the key role in the catalyst activity and product selectivity. The experimental data over fresh SAPO-34 are given in Table 2. The kinetic data were obtained under the following conditions: temperature, 450, 475, and 490 °C; weight hour space velocity, between 30 and 955 $g_{MeOH}\ g_{cat}^{-1}\ h^{-1}$; water/methanol molar ratio in the feed, 0, 2 and 4.

#### 2.3.1. *Effect of reaction temperature*

Fig. 1 shows the effect of temperature on the product distribution, the results correspond to pure methanol feed. As observed, methanol concentration decreases notably with increasing temperature (Fig. 1a), which is due to the enhanced methanol consumption rate at higher temperature. Complete methanol conversion reaches at a methanol weight hour space velocity of 31.8 $g_{MeOH}\ g_{cat}^{-1}\ h^{-1}$, in accordance with the data obtained by Bos et al. (1995), with a value of 50 $g_{MeOH}\ g_{cat}^{-1}\ h^{-1}$. The deviation between these two experiments is rational since Bos et al. used pure SAPO-34 zeolite in the kinetic study, while the DMTO catalyst is prepared by agglomerating the SAPO-34 zeolite with other inert charges. Wu et al. (2004) found temperature was the strongest factor that affects ethylene/propylene ratio. Different ethylene/propylene ratios can be obtained by adjusting reaction temperature. This is in agreement with the experimental data (Fig. 1b), as ethylene concentration increases with temperature while the change in propylene concentration (Fig. 1c) is not very significant. An explanation of these observations can possibly be the intensified cracking rate of higher hydrocarbons as temperature increases, or just the inherent characteristic of the MTO reaction with more ethylene formed directly from methanol at higher temperature. The later is proved by the yield-conversion plot (Fig. 2). In contrast to the trend for ethylene, the decrease in temperature favors formation of sum $C_4$ (Fig. 1d) and the rest hydrocarbon (Fig. 1e), with a value of 16.9 wt% and 11.7 wt% respectively for 450 °C under complete methanol conversion.

The yield-conversion plot provides direct information for distinguishing the type of product (stable or intermediate) (Abbot and Wojciechowski, 1985; Chen et al., 2007). The olefin yields are plotted against methanol conversion at temperatures of 450, 475, and 490 °C in Fig. 2. Interestingly, the curves of the yields of $C_2$–$C_4$ olefins against methanol conversion are almost straight lines for all the reaction conditions, indicating that the olefins formed over SAPO-34 catalyst are stable primary products. Therefore, the secondary reactions of the olefins could be safely ignored in the kinetic model. The same trend appears in methane and propane, with a little deviation for sum $C_5^+$. For the MTO reaction taken over SPAO-34 catalyst, the maximum selectivity to $C_2$–$C_4$ olefins approaches 90 wt% on a dry gas base (Wei et al., 2012), with some minor products such as methane, ethane, propane and $C_5$+ hydrocarbons, thus the secondary reaction of $C_5$+ will not be very important. Finally, a parallel kinetic scheme should be suitable for MTO reaction (Gayubo et al., 2000).

#### 2.3.2. *Effect of water content*

Gayubo took comprehensive studies of the effect of water content in the feed on the MTO reaction over different types of catalysts (SAPO-n (Gayubo et al., 2007, 2000), ZSM-5 (Gayubo et al., 2002)), the resistance to the reaction rates due to the presence of water in the reaction medium has been observed in their experiments. This may be the result of competitive adsorption of water and methanol molecules in the active sites. As water content is increased in the feed, the available active sites for methanol are correspondingly reduced, thus leading to a lower methanol consumption rate. There different water/methanol molar ratios in the feed 0, 2, and 4 (corresponding to water content in the feed of 0, 0.53 and 0.69), have been used in the experiment. Methanol conversion at various water content is shown in Fig. 3. Clearly, the presence of water in the feed exerts considerable influence on the total methanol reaction rate.

#### 2.3.3. *Effect of coke content*

The effect of coke content derived from the 'cigar burn' time evolution of the catalyst bed on the performance of the MTO

**Table 2 – Experimental data over fresh SAPO-34 catalyst.**

| | | Product distribution ($CH_2$ basis) | | | | | | |
|---|---|---|---|---|---|---|---|---|
| | WHSV ($g_{MeOH}\ g_{cat}^{-1}\ h^{-1}$) | $CH_4$ | $C_2H_4$ | $C_3H_6$ | $C_3H_8$ | $C_4$ | $C_5^+$ | MeOH |
| | $H_2O$:MeOH (mol) = 0:1 | | | | | | | |
| 450 °C | 955.0 | 0.21 | 5.90 | 9.75 | 0.73 | 3.00 | 0.74 | 79.68 |
| | 477.5 | 0.56 | 10.48 | 16.47 | 1.34 | 5.09 | 1.18 | 64.88 |
| | 191.0 | 0.63 | 21.02 | 31.87 | 2.15 | 9.96 | 3.04 | 31.33 |
| | 95.5 | 0.82 | 24.49 | 36.72 | 2.69 | 12.40 | 4.96 | 17.92 |
| | 47.8 | 1.03 | 28.24 | 42.25 | 3.35 | 15.73 | 7.38 | 2.02 |
| | 31.8 | 0.95 | 28.59 | 42.00 | 3.54 | 16.91 | 7.29 | 0.73 |
| 475 °C | 955.0 | 0.34 | 7.67 | 11.11 | 0.77 | 3.19 | 0.95 | 75.97 |
| | 477.5 | 0.46 | 12.67 | 18.28 | 1.18 | 5.52 | 1.91 | 59.99 |
| | 191.0 | 0.88 | 24.47 | 33.37 | 2.19 | 9.45 | 3.92 | 25.73 |
| | 95.5 | 0.99 | 30.51 | 39.42 | 2.03 | 12.48 | 4.71 | 9.86 |
| | 47.8 | 1.07 | 31.77 | 42.25 | 2.54 | 14.70 | 6.26 | 1.43 |
| | 31.8 | 1.12 | 32.30 | 41.88 | 2.63 | 14.95 | 6.64 | 0.50 |
| 490 °C | 955.0 | 0.40 | 8.24 | 10.97 | 0.71 | 3.08 | 1.00 | 75.61 |
| | 477.5 | 0.67 | 15.87 | 21.44 | 1.44 | 5.92 | 2.18 | 52.48 |
| | 191.0 | 1.18 | 24.80 | 33.18 | 2.13 | 10.32 | 4.67 | 23.73 |
| | 95.5 | 1.18 | 30.51 | 39.41 | 2.22 | 12.67 | 5.83 | 8.18 |
| | 47.8 | 1.35 | 31.47 | 41.76 | 2.59 | 14.29 | 7.07 | 1.47 |
| | 31.8 | 1.41 | 31.64 | 41.72 | 2.85 | 14.91 | 7.00 | 0.47 |
| | $H_2O$:MeOH (mol) = 2:1 | | | | | | | |
| 450 °C | 498.8 | 0.15 | 4.50 | 6.08 | 0.24 | 1.76 | 1.29 | 85.98 |
| | 199.5 | 0.46 | 12.17 | 17.56 | 1.03 | 5.56 | 3.45 | 59.78 |
| | 99.8 | 0.77 | 19.82 | 27.61 | 1.69 | 9.24 | 5.29 | 35.58 |
| | 49.9 | 1.09 | 25.55 | 35.31 | 2.26 | 12.26 | 7.67 | 15.87 |
| 475 °C | 498.8 | 0.29 | 7.44 | 9.22 | 0.41 | 2.59 | 1.41 | 78.65 |
| | 199.5 | 0.57 | 15.06 | 18.24 | 1.01 | 5.41 | 2.73 | 56.98 |
| | 99.8 | 0.94 | 24.76 | 31.34 | 1.90 | 9.78 | 5.00 | 26.29 |
| | 49.9 | 1.10 | 29.44 | 38.33 | 2.41 | 12.29 | 5.19 | 11.23 |
| 490 °C | 498.8 | 0.39 | 9.04 | 10.86 | 0.48 | 3.06 | 1.50 | 74.66 |
| | 199.5 | 0.77 | 18.34 | 22.09 | 1.30 | 6.64 | 3.17 | 47.70 |
| | 99.8 | 0.99 | 26.99 | 31.68 | 1.72 | 9.41 | 4.08 | 25.15 |
| | 49.9 | 1.20 | 31.90 | 39.04 | 2.39 | 11.80 | 4.57 | 9.10 |
| | $H_2O$:MeOH (mol) = 4:1 | | | | | | | |
| 450 °C | 505.5 | 0.28 | 4.87 | 7.58 | 0.49 | 2.52 | 1.31 | 82.95 |
| | 202.2 | 0.59 | 10.52 | 16.13 | 1.37 | 5.58 | 2.96 | 62.86 |
| | 101.1 | 0.90 | 18.35 | 25.61 | 2.34 | 8.90 | 4.15 | 39.74 |
| | 50.6 | 0.96 | 25.68 | 36.49 | 2.66 | 12.38 | 4.84 | 16.98 |
| | 33.7 | 1.35 | 24.46 | 39.08 | 3.43 | 13.89 | 6.15 | 11.63 |
| 475 °C | 505.5 | 0.32 | 7.14 | 9.81 | 0.51 | 2.97 | 1.17 | 78.08 |
| | 202.2 | 0.57 | 13.66 | 19.25 | 1.64 | 6.22 | 2.47 | 56.18 |
| | 101.1 | 0.90 | 21.37 | 29.64 | 2.26 | 9.64 | 3.83 | 32.38 |
| | 50.6 | 1.15 | 26.78 | 37.16 | 2.73 | 12.05 | 4.77 | 15.35 |
| 490 °C | 505.5 | 0.36 | 7.41 | 8.73 | 0.51 | 2.52 | 1.18 | 79.29 |
| | 202.2 | 0.62 | 16.22 | 18.80 | 1.02 | 5.56 | 2.76 | 55.02 |
| | 101.1 | 0.99 | 24.48 | 30.02 | 1.77 | 9.37 | 3.81 | 29.57 |
| | 50.6 | 1.24 | 29.23 | 36.13 | 2.22 | 11.24 | 4.96 | 14.98 |

reaction maybe unrepresentative (Haw and Marcus, 2005). Ideally the coke distribution rather than average coke content should be involved in the kinetic model. By taking photographs of the catalyst during the course of the methanol reaction over phosphorous modified ZSM-5 catalyst, Kaarsholm et al. (2007) observed three distinct coking patterns. Compared to the ZSM-5 catalyst, the coke distribution would be more obvious in the SAPO-34 catalyst because of fast coking rate and negligible secondary reactions. Therefore, it is extremely hard to measure the coke content in the fixed bed reactor. Fortunately, it is argued that in a batch fluidized bed reactor, due to the well mixing of catalyst, the coke content on the catalyst is more uniform than in a fixed bed reactor (Wei et al., 2012).

Coke behavior in a batch fluidized bed reactor is shown in Fig. 4. As can be seen, the rate of coke deposition is rapid at the initial stage followed by a gradual decrease. This can be attributed to the product shape selectivity in the SAPO-34 catalyst (Hereijgers et al., 2009). The final coke content reaches at a value of 9.3 wt%. Wei et al. (2012) studied methanol conversion over DMTO catalyst by using a tapered element oscillation microbalance (TEOM) for the simultaneous measurement of coke deposition. They found that the maximum

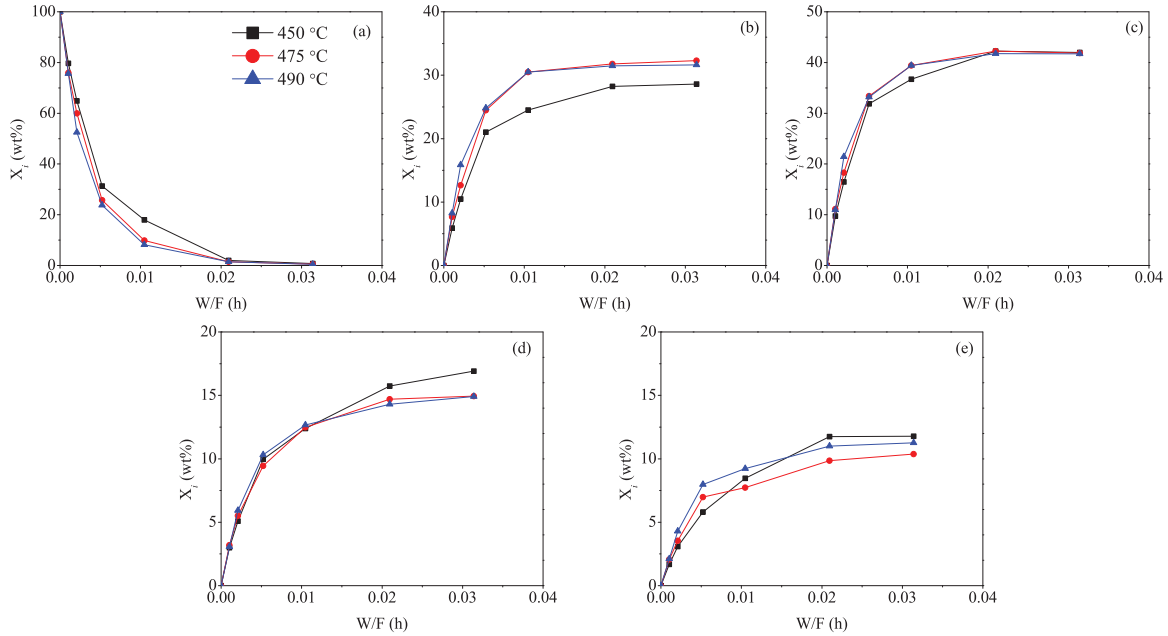


**Fig. 1 – Effect of reaction temperature on the evolution with space time of the product mass fraction. (a) Methanol; (b) ethylene; (c) propylene; (d) $C_4$; (e) rest hydrocarbons. Water content in the feed $X_W = 0$.**

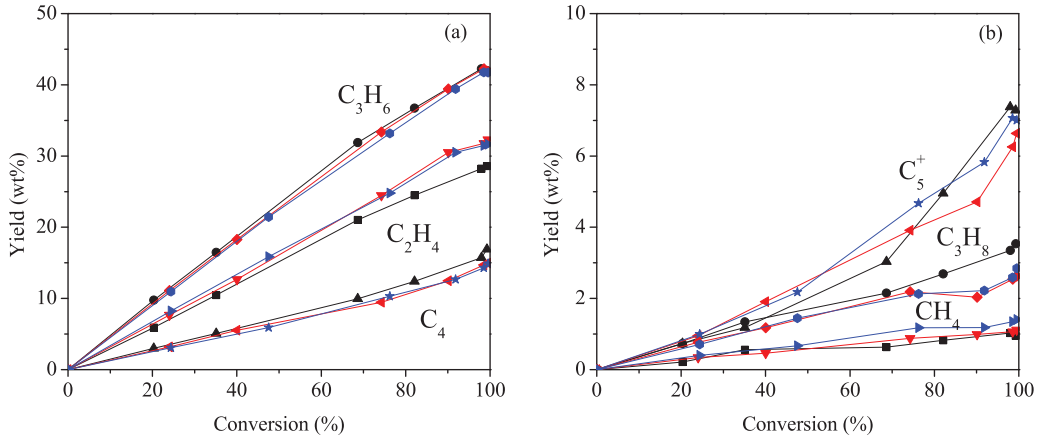


**Fig. 2 – Evolution of product yields with methanol conversion for different temperatures. ■, 450 °C; ▼, 475 °C; ▲, 490 °C; water content in the feed $X_W = 0$. Graph (a) $C_2$–$C_4$ olefins; graph (b) methane, propane and $C_5^+$.**

coke content was almost the same (around 9.5 wt%) for the temperature range between 450 and 500 °C, which is in accordance with the result in this study. The consistency between these two experiments indicate that the operation mode (fixed bed or fluidized bed) has no influence on the catalyst deactivation characteristic, except for the coke distribution, i.e. non-uniform coke in fixed bed and uniform coke in fluidized bed.

Fig. 5 shows the effect of coke content on the product distribution. The maximum ethylene and light olefins fraction reach at a coke content of 7.8 wt%, with a value of 52 wt% and 86 wt%, respectively, indicating a certain amount of coke

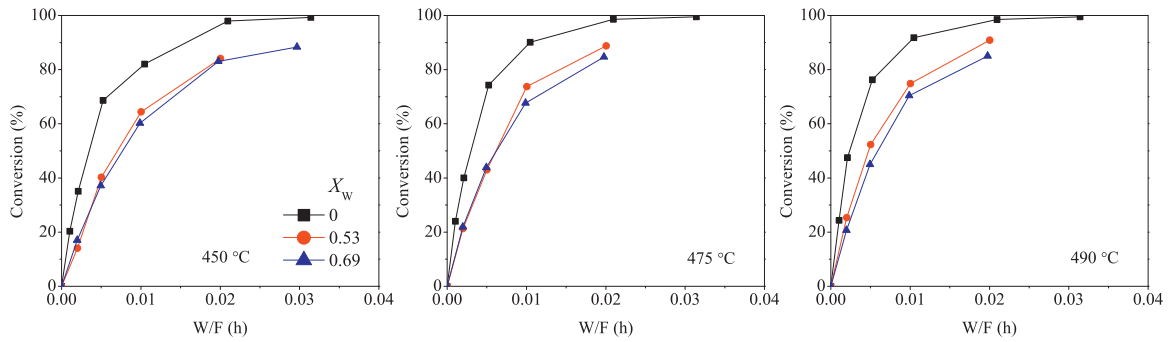


**Fig. 3 – Effect of water content in the feed on the methanol conversion. Temperature: graph (a) 450 °C; graph (b) 475 °C; graph (c) 490 °C.**

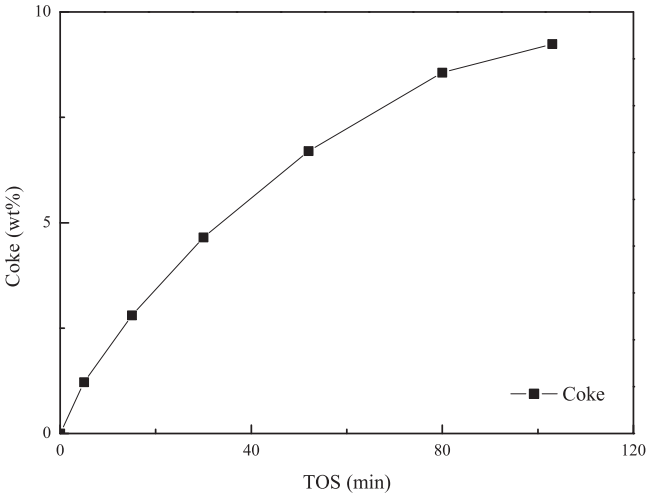


**Fig. 4 – Evolution with time on stream of the coke content in a fluidized bed reactor at 480 °C, pure methanol in the feed, no regeneration, and WHSV of 2.54 $g_{MeOH}\ g_{cat}^{-1}\ h^{-1}$.**

accumulated in the catalyst is preferred for the MTO reaction. Moreover, a sudden decrease in methanol conversion and product yield are observed when the coke content exceeds 7.8 wt%. Qi et al. (2007) studied coke behavior in the SAPO-34 catalyst, abrupt change in the methanol conversion was obtained at a coke content of 5.7 wt%, much lower than this work, which indicates that the value depends on the catalyst property, more accurately, depends on the content of SAPO-34 zeolite in the catalyst. The deactivation of the SAPO-34 catalyst can be explained by two mechanisms: pore blockage and active site coverage (Guisnet, 2002). First, the increase of coke content greatly inhibits molecular diffusion in the pore channel, and a more intense restriction for larger molecules can be expected, leading to the selective deactivation in the MTO process. Second, the active sites for methanol transformation are gradually decreased when covered by the coke, resulting in a lower catalyst activity. These two phenomena together influence methanol conversion and product selectivity.

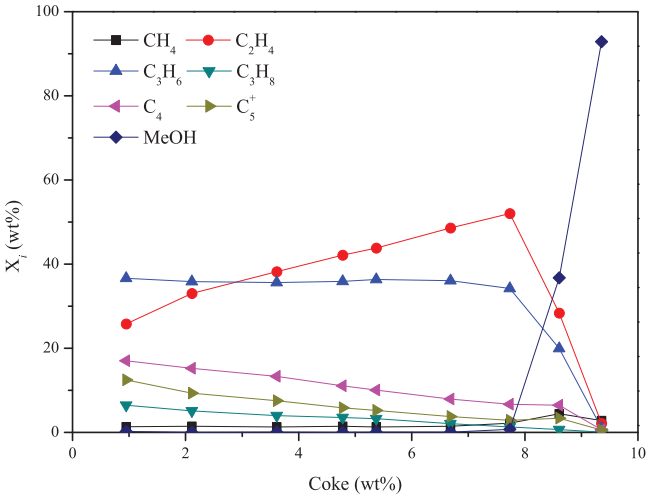


**Fig. 5 – Effect of coke content on the product distribution at 480 °C, pure methanol in the feed and WHSV of 2.54 $g_{MeOH}\ g_{cat}^{-1}\ h^{-1}$.**

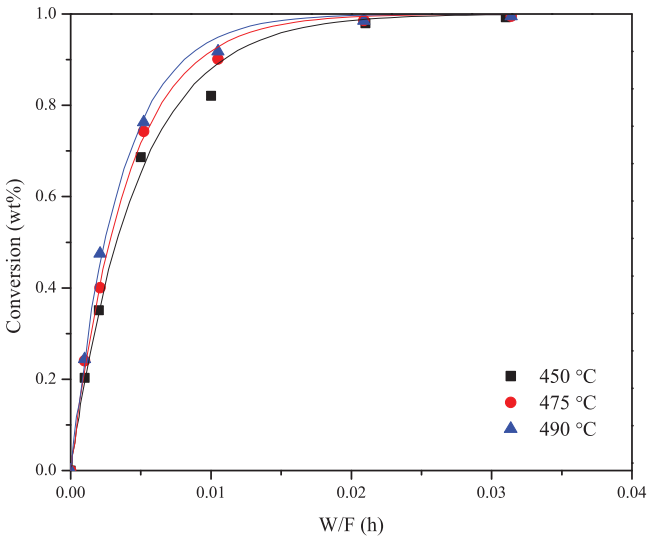


**Fig. 6 – Effect of temperature on the methanol conversion, water content in the feed $X_W = 0$. Lines, calculated with the kinetic model. Points, experimental results.**

## 3. Kinetic model

### 3.1. *Main reactions*

#### 3.1.1. *Reaction order*

The mass conservation equation for a plug flow reactor can be expressed as

$$\frac{dX}{dW/F_{MeOH}} = k_t(1-X)^n \quad (1)$$

where X is the methanol conversion; $F_{MeOH}$ is the methanol flow rate in the feed, $g\,h^{-1}$; and $k_t$ is total methanol reaction rate, $g_{MeOH}\ g_{cat}^{-1}\ h^{-1}$. The calculated results show the best agreement with the experimental data when the reaction order *n* is set at 1 (Fig. 6), this means that the kinetic equation is of first order with respect to the methanol concentration.

#### 3.1.2. *Reaction network*

The elaborated model proposed by Bos et al. (1995) captures the key characteristics of the MTO reaction and suitably fits the experimental data obtained in a fixed bed microreactor. However, the secondary reactions of propylene and $C_4$ considered in the model have been proven to be not important in this work. Thus a simplification has been made (Fig, 7). In short, the products are grouped into seven lumps (1) methane, (2) ethylene, (3) propylene, (4) propane, (5) $C_4$, (6) $C_5^+$ (including $C_5$, $C_6$ hydrocarbons and ethane) and (7) coke. Step 7 is eliminated in this section because the kinetic data has been obtained under particularly small time on stream with negligible coke formation.

#### 3.1.3. *Kinetic parameters*

The detailed kinetic model for each lump can be described by:

$$\frac{dX_i}{dW/F_{MeOH}} = R_i \quad (2)$$

The formation rate of each lump, $R_i$, is

$$R_{CH_4} = k_1\theta_W C_{MeOH} Mw_{CH_4} \quad (3)$$

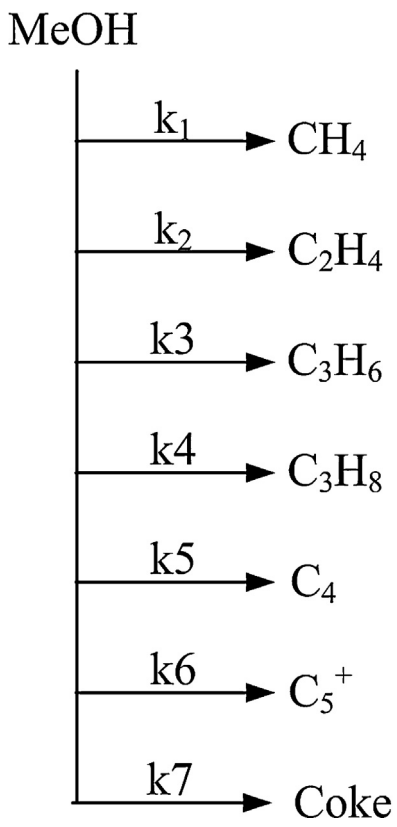


**Fig. 7 – Kinetic scheme for the MTO reaction.**

$$R_{C_2H_4} = 1/2 \times k_2\theta_W C_{MeOH} Mw_{C_2H_4} \quad (4)$$

$$R_{C_3H_6} = 1/3 \times k_3\theta_W C_{MeOH} Mw_{C_3H_6} \quad (5)$$

$$R_{C_3H_8} = 1/3 \times k_4\theta_W C_{MeOH} Mw_{C_3H_8} \quad (6)$$

$$R_{C_4} = 1/4 \times k_5\theta_W C_{MeOH} Mw_{C_4} \quad (7)$$

$$R_{C_5^+} = 1/5 \times k_6\theta_W C_{MeOH} Mw_{C_5} \quad (8)$$

The total reaction rate for methanol and water has the following expressions:

$$R_{MeOH} = -\left(\sum_1^6 k_i\theta_W\right) C_{MeOH} Mw_{MeOH} \quad (9)$$

$$R_{H_2O} = \left(\sum_1^6 k_i\theta_W\right) C_{MeOH} Mw_{H_2O} \quad (10)$$

where $C_{MeOH}$ is the methanol concentration, (mol $L^{-1}$); $Mw$ is the molar weight, (g $mol^{-1}$); $X_i$ denotes the mass fraction (on a water present basis) of each lump and $k_i$ is the reaction rate corresponding to lump $i$, L $g_{cat}^{-1}$ $min^{-1}$. The effect of water content in the reaction medium on the attenuation of individual kinetic step has been taken into account by multiplying the kinetic constant with the term $\theta_W$,

$$\theta_W = \frac{1}{1 + K_W X_W} \quad (11)$$

The parameter $K_W$ has been assumed to be same for all the lumps in the kinetic model and $X_W$ is the water mass fraction in the reaction medium (on a water present basis). To reduce the strong correlation between frequency factor and activation energy, a reparametrized Arrhenius equation has been used by expressing the kinetic constant $k_i$ to its corresponding value $k_{i0}$ at a reference temperature, 723.15 K,

$$k_i = k_{i0} \exp\left(-\frac{Ea_i}{R}\left(\frac{1}{T} - \frac{1}{723.15}\right)\right) \quad (12)$$

The estimation of the kinetic parameters has been based on the nonlinear least-squares Levenberg–Marquardt (Marquardt, 1963) method by minimizing an objective function:

$$OF = \sum_{i=1}^{n}\sum_{j=1}^{m} w_{ij}\left(X_{i,j} - X_{i(calc),j}\right)^2 \quad (13)$$

where $w_{ij}$ is the weighting factor, $X_{i,j}$ is the measured mass fraction of lump $i$ at experimental condition $j$, and $X_{i(calc),j}$ is the corresponding mass fraction calculated from the solution of the mass conservation equations.

The calculated kinetic parameters of best fit to the experimental data are listed in Table 3. The corresponding value of the objective function, Eq. (13), is 0.0735. It is worth to mention that the calculated activation energy for propane is 13.45 kJ $mol^{-1}$, much lower than the other reactions. Possible explanation is the reaction tends to generate more propane at a lower temperature (Wei et al., 2012). Figs. 8 and 9 show the experimental and calculated mass fraction (water free basis) for each lump. As can be seen, the model fits the experimental data generally well for all the reaction conditions.

### 3.2. *Catalyst deactivation*

For the industrial MTO reactor, the deactivation should be highly concerned, since the spent catalyst is regenerated continuously at a partial coke combustion mode in order to achieve high selectivity of ethylene and propylene. For this reason, the deactivation kinetic model of MTO reaction is of great importance.

#### 3.2.1. *Deactivation model*

By taking into account the effect of coke content on the reaction rate, the formation rates of hydrocarbons and coke are updated according to the following expression:

$$R_i = \nu_i k_i \theta_W C_{MeOH} \varphi_i Mw_i \qquad i = 1 - 7 \quad (14)$$

where $\nu_i$ is the stoichiometric number and $\varphi_i$ is the deactivation function. Different empirical deactivation correlations proposed by Froment et al. (2010) have been tested in our model but all failed in reproducing the rapid decreasing in catalyst activity when methanol breakthrough occurs. Nayak et al. (2005) used Eq. (15) to relate catalyst activity to the coke deposition on catalyst:

$$\varphi = \frac{A + 1}{A + \exp(BC_c)} \quad (15)$$

Here $A$ and $B$ are constants, and $C_C$ is the weight percent of coke on the catalyst, (g 100 $gcat^{-1}$). Eq. (15) can characterize the sharp decrease of catalyst activity with increasing coke content $C_c$. This trend is somewhat similar with the MTO process, of which the catalyst activity stays steady at the initial stage followed by a fast deactivation. However, this equation fails to reflect the selective deactivation in the MTO process since

**Table 3 – Kinetic parameters.**

| *Kinetic constant (L $g_{cat}^{-1}$ $min^{-1}$) | $k_{i0}$ (at 450 °C) | $Ea_i$ (kJ $mol^{-1}$) | Deactivation constant $\alpha_i$ | Water effect |
|---|---|---|---|---|
| $k_1$ | 0.10 | 117.7 | 0.06 | $\theta_W =$ |
| $k_2$ | 4.93 | 56.9 | 0.14 | $1/1 +$ |
| $k_3$ | 7.32 | 41.9 | 0.21 | $K_W X_W$ |
| $k_4$ | 0.52 | 13.4 | 0.20 | |
| $k_5$ | 2.60 | 31.2 | 0.24 | |
| $k_6$ | 1.02 | 45.8 | 0.27 | |
| $k_7$ | 2.31 | 53.3 | 0.31 | |
| $K_W$ | 3.05 | | | |

* $k_i = k_{i0} \exp\left(-\frac{Ea_i}{R}\left(\frac{1}{T} - \frac{1}{723.15}\right)\right)$

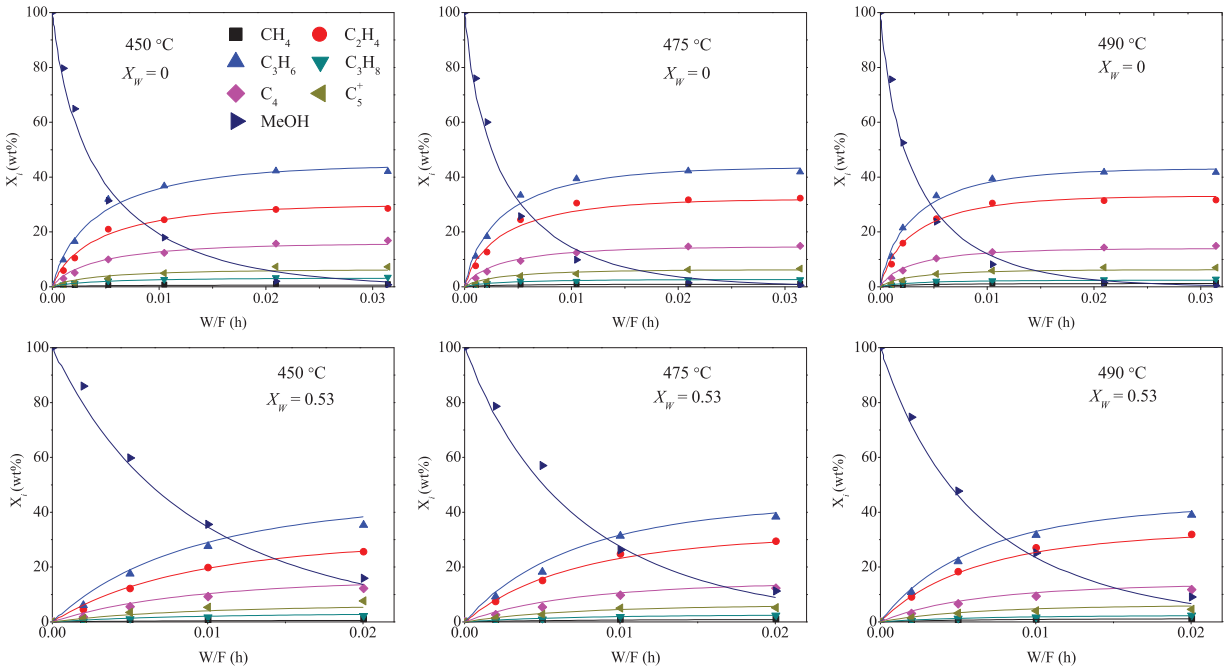


**Fig. 8 – Comparison between the experimental and calculated mass fraction of each lump at different temperatures and water contents. Lines, calculated with the kinetic model; points, experimental results. Upper graph: water content in the feed, $X_W = 0$; lower graph: water content in the feed, $X_W = 0.53$.**

A and B are constants for all the reactions. Thus we add an exponential correlation to quantify the selective deactivation:

$$\varphi_i = \frac{1}{1 + A\exp(B \times (C_c - D))} \exp(-\alpha_i C_c) \quad (16)$$

where D is the *critical coke content*, the value of which depends on the catalyst property. The first part in Eq. (16) stands for the abrupt decreasing trend of catalyst activity when coke content exceeds the *critical coke content*, while the second part is used to represent the selective deactivation. Note that $\alpha_i$ is a reaction-dependent parameter, i.e., it has different values for different reactions. The effect of coke content on product selectivity can then be modeled by taking different $\alpha_i$ in Eq. (16).

### 3.2.2. *Calculation of deactivation parameters*

Compared to the contact time needed for the complete conversion of methanol, the time for buildup of coke on the catalyst is considerably large. Thus the pseudo-steady state

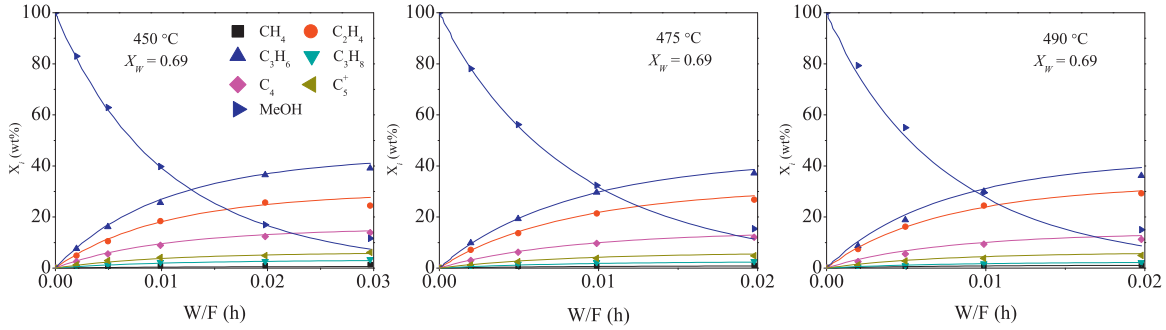


**Fig. 9 – Comparison between the experimental and calculated mass fraction of each lump at different temperatures and a feed with 69 wt% water. Lines, calculated with the kinetic model; points, experimental results.**

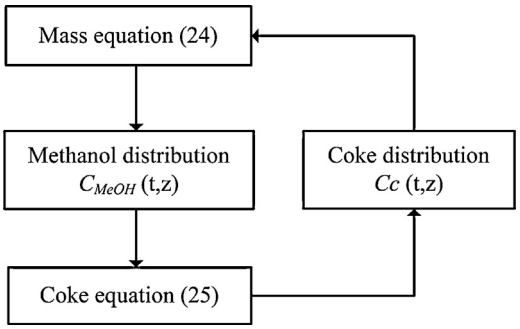


**Fig. 10 – Mathematical procedure for the calculation of deactivation parameters.**

approximation for the gas phase may be applied, and the same mass conservation equations as described above can be used:

$$\frac{\partial X_i}{\partial z} = \frac{W}{F_{MeOH}} R_i \tag{17}$$

While the coke deposition (denoted by $(CH_2)_n$) on the catalyst changes both in the time on stream and space, it can be described by a differential equation:

$$\frac{\partial C_C(t,z)}{\partial t} = 100 M_{WCH_2} \cdot R_7(t,z) \tag{18}$$

Note that the term $R_7$ is related to the axial position. Therefore, the catalyst coke content at different axial positions for different times on stream can be calculated through Eq. (18). The calculation procedure is shown in Fig. 10.

For simplicity, the reaction time was first discretized; the gas phase composition along the catalyst bed was calculated from the mass conservation Eq. (17) at a corresponding time t; Eq. (18) was then invoked to calculate coke distribution, which could be used in Eq. (17) for the next time step. The loop would end at a predefined time on stream. The deactivation parameters of best fit to the experimental data were obtained according to Eq. (13).

The deactivation function proposed was aimed at quantifying the abrupt decreasing trend and selective deactivation in the MTO process, thus $D$ and $\alpha_i$ are the key parameters. Actually $D$ represents the *critical coke content* at which a sharp decrease in catalyst activity appears. As is shown in the batch fluidized bed result, it has been found in our experiments that when coke content exceeds 7.8 wt% a sharp change of catalyst activity and product selectivity will be expected. Therefore, in this work, $D$ is set as 7.8; the number is a characteristic value for DMTO catalyst. Parameter A determines the value of the deactivation correlation when catalyst coke content reaches the critical point $D$, while $B$ affects the deactivation curve's gradient. It was found that when $A$ and $B$ were set as 9 and 2 respectively best fit the experiment. The final kinetic parameters of best fit are shown in Table 3. As expected, the deactivation constants for olefins increase with increasing characteristic molecular size of the corresponding lumps, i.e., the larger the molecular, the higher the deactivation rate. This is in agreement with the product shape selectivity in the MTO reaction over SAPO-34 catalyst.

Figs. 11 and 12 show the comparison of the evolution of the experimental and calculated product composition (water free basis) for different reaction conditions. The lines correspond to the values calculated using the kinetic model and the points referred to the experimental results.

The effect of temperature on the evolution of effluent methanol mass fraction with time on stream is shown in Figs. 11d and 12c and f. The graph corresponds to weight hour space velocity of 2.1 $g_{MeOH}\, g_{cat}^{-1}\, h^{-1}$ and 20 wt% water in the feed. As observed, the catalyst life time (corresponding to methanol conversion of 99 wt%) decreases with increasing temperature, with a value 62 min at 450 °C, 58 min at 475 °C and 54 min at 490 °C, which is because of the enhanced coke deposition rate by increasing temperature.

The effect of water content on the attenuation of catalyst activity is validated by comparing the evolution of methanol concentration with time on stream in Fig. 12a and c (475 °C). The time for methanol breakthrough changes from 52 min for pure methanol feed to 68 min for 20 wt% water content in the feed. Similarly, the same trend appears at temperature of 490 °C (Fig. 12d and f).

### 3.3. *Evaluation of fixed bed reactor*

A comprehensive mathematical model for dynamic fixed bed reactor has been solved using Comsol Multiphysics software with embedded models, the Transport of Diluted Species model for gaseous components, and the Domain ODEs and DAEs model for solid phase. The material balance is described by the equation:

$$\frac{\partial C_i(t,z,r)}{\partial t} + \nabla \cdot (-D_i \cdot \nabla C_i(t,z,r)) + \nabla (\mathbf{u} C_i(t,z,r)) = R_i(t,z,r) \tag{19}$$

$$\frac{\partial C_C(t,z,r)}{\partial t} = 100 M_{WCH_2} \cdot R_7(t,z,r) \tag{20}$$

The coke distribution is calculated via Eq. (20). The initial conditions are

$$t = 0,\ C_i(0,z,r) = C_0,\ C_C(0,z,r) = 0, \tag{21}$$

and boundary conditions are

$$z = 0,\ C_i(t,0,r) = C_0; \quad z = L,\ \frac{\partial C_i(t,z,r)}{\partial z} = 0, \tag{22}$$

and

$$r = 0,\ \frac{\partial C_i(t,z,r)}{\partial r} = 0; \quad r = R,\ \frac{\partial C_i(t,z,r)}{\partial r} = 0. \tag{23}$$

The diffusion coefficients were adopted from Keil et al. (1999): $5.21 \times 10^{-10}\ m^2\ s^{-1}$ for water and $3.89 \times 10^{-10}\ m^2\ s^{-1}$ for methanol. The diffusion coefficients for all hydrocarbon species are assumed to be the same, i.e. $6.62 \times 10^{-9}\ m^2\ s^{-1}$. For simplicity, the difference between the diffusion coefficients at axial and radial direction has not been taken into account. The mass fraction of methanol, ethylene and propylene at different times on stream along the axial direction, together with the catalyst coke content, are displayed in Fig. 13. The simulation has been carried out at temperature of 475 °C, weight hour space velocity of 2.08 $g_{MeOH}\, g_{cat}^{-1}\, h^{-1}$ and a feed with 20 wt% water. The predicted results for product concentrations agree with the experimental data reasonably well. The relative deviations for major species are less than 5.0% (1.9% for ethylene, 2.0% for propylene, 4.6% for butylenes, and 1.4% for methanol). The largest deviation comes from the prediction of minor species methane. The reasons may be that (1) methane is not formed from hydrocarbon pool mechanism; (2) experimental error in GC analysis since methane concentration is

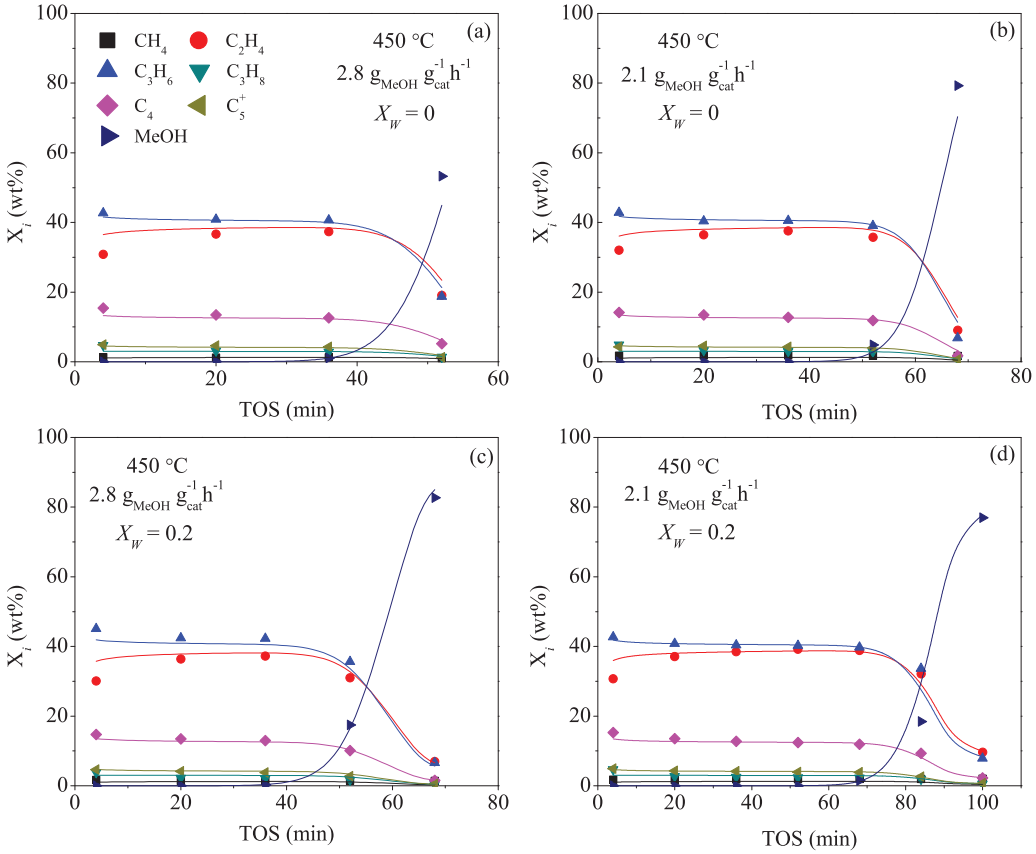


**Fig. 11 – Comparison of the evolution with time on stream of the experimental and calculated mass fraction of each lump at 450 °C. Lines, calculated with the kinetic model; points, experimental results.**

low at reaction conditions; and (3) a small amount of methanol cracks and produces methane at high temperature. In general, the large deviation of the methane concentration will not affect the accuracy of the kinetic model as the methane concentration is very low and plays a minor role in the kinetic behavior of methanol reaction over SAPO-34 catalyst. It is observed that, methanol could be completely converted with a considerably small fraction of catalyst (Fig. 13a). There is a spatially inhomogeneous aging of the catalyst along the catalyst bed (Fig. 13d). Coke first accumulates in the upstream of the feed flow with catalyst downstream totally undeactivated. Then the coke deposition moves downward leaving deactivated catalyst in its wake as reaction proceeds. The deactivation in catalyst changes the concentration profile of

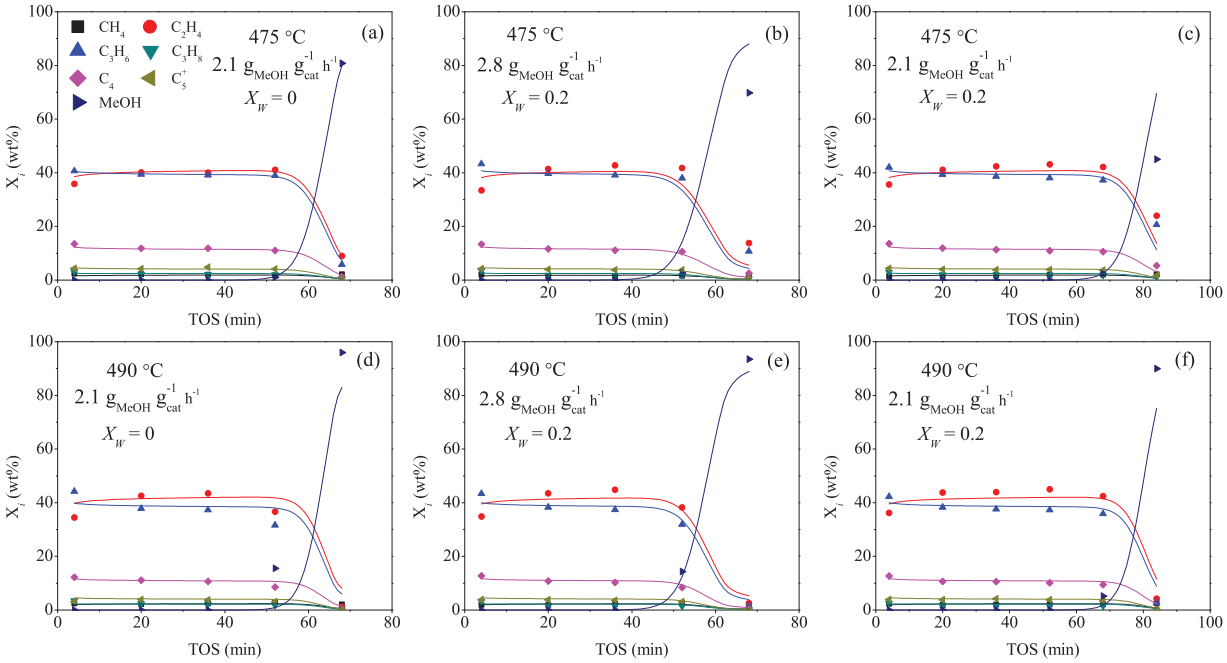


**Fig. 12 – Comparison of the evolution with time on stream of the experimental and calculated mass fraction of each lump at 475 and 490 °C. Lines, calculated with the kinetic model; points, experimental results.**

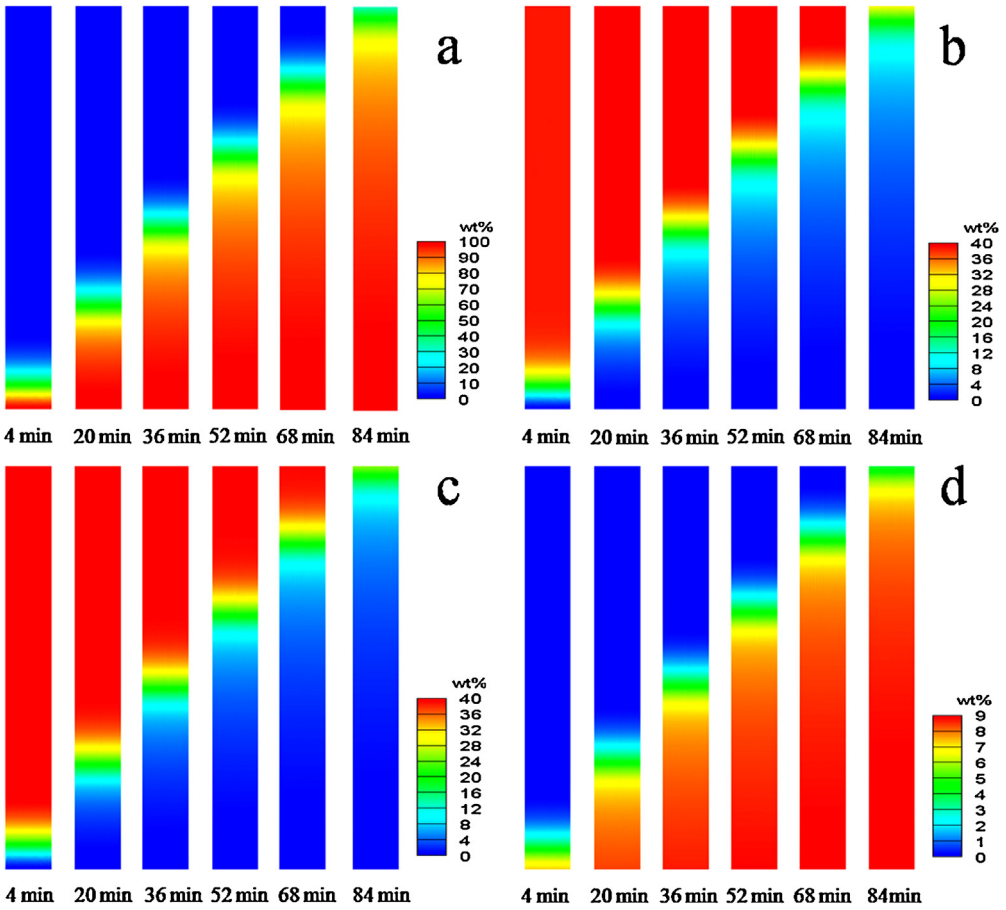


**Fig. 13 – Concentration profile of (a) methanol; (b) ethylene; (c) propylene and (d) coke content along the axial direction at different times on stream. Simulation conditions: temperature, 475 °C; WHSV = 2.08 $g_{MeOH}\ g_{cat}^{-1}\ h^{-1}$ and water content in the feed, $X_W = 0.2$.**

ethylene and propylene (Fig. 13b and c). When the catalyst in the bed approaches heavily deactivated, coke distribution along the bed height reaches uniform.

## 4. Conclusion

MTO process has been recently industrialized, and will become one of the main streams of light olefins production. In this work, we have studied the kinetics for MTO reaction over industrial MTO catalyst, i.e. DMTO catalyst, in a fixed bed reactor.

Experimental results for the MTO reaction suggest that methanol reaction rate is affected by the temperature and water content. An increase in the reaction temperature intensifies the methanol consumption rate, while the water introduced in the feed attenuates the reactions. A linear dependence between product yields and methanol conversion indicates that the primary hydrocarbon products are parallel formed from methanol. Therefore a kinetic model with seven lumps (i.e. methane, ethylene, propylene, propane, $C_4$, $C_5^+$ and coke) has been established, where all the reaction rates are assumed to be first order in methanol concentration. Note that the coke content on catalyst not only affect the methanol conversion but also has a direct impact on the product distribution due to the shape selectivity, a selective catalyst deactivation model was proposed. In fixed bed reactor, meanwhile, the coke deposited on catalyst shows a distribution along the catalyst bed as demonstrated by Kaarsholm et al. (2007). The average coke content cannot reflect such a distribution in fixed bed reactor. Therefore, a batch fluidized bed reactor was used to obtain more deatiled data on catalyst deactivation as it has the advantage in building up a uniform coke distribution due to the excellent solid mixing performance. This model shows to fit the experimental data in the fixed bed reactor generally well, with the relative deviations less than 5% for the major species such as ethylene, propylene, butylenes, and methanol.

## Acknowledgement

This work is supported by the National Natural Science Foundation of China (Grant no. 91334205), and the Strategic Priority Research Program of the Chinese Academy of Sciences (Grant no. XDA07070100)

## References

Abbot, J., Wojciechowski, B., 1985. Catalytic cracking and skeletal isomerization of *n*-hexene on ZSM-5 zeolite. Can. J. Chem. Eng. 63, 451–461.

Aitani, A., Yoshikawa, T., Ino, T., 2000. Maximization of FCC light olefins by high severity operation and ZSM-5 addition. Catal. Today 60, 111–117.

Alvaro-Munoz, T., Marquez-Alvarez, C., Sastre, E., 2012. Use of different templates on SAPO-34 synthesis: effect on the

acidity and catalytic activity in the MTO reaction. Catal. Today 179, 27–34.
Alwahabi, S.M., Froment, G.F., 2004. Single event kinetic modeling of the methanol-to-olefins process on SAPO-34. Ind. Eng. Chem. Res. 43, 5098–5111.
Benito, P.L., Gayubo, A.G., Aguayo, A.T., Castilla, M., Bilbao, J., 1996. Concentration-dependent kinetic model for catalyst deactivation in the MTG process. Ind. Eng. Chem. Res. 35, 81–89.
Bleken, F., Bjørgen, M., Palumbo, L., Bordiga, S., Svelle, S., Lillerud, K.-P., Olsbye, U., 2009. The effect of acid strength on the conversion of methanol to olefins over acidic microporous catalysts with the CHA topology. Top. Catal. 52, 218–228.
Bos, A.N.R., Tromp, P.J.J., Akse, H.N., 1995. Conversion of methanol to lower olefins—kinetic modeling, reactor simulation, and selection. Ind. Eng. Chem. Res. 34, 3808–3816.
Cavani, F., Trifiro, F., 1995. The oxidative dehydrogenation of ethane and propane as an alternative way for the production of light olefins. Catal. Today 24, 307–313.
Chang, C.D., 1980. A kinetic model for methanol conversion to hydrocarbons. Chem. Eng. Sci. 35, 619–622.
Chang, C.D., Lang, W.H., Silvestri, A.J., 1977. Manufacture of light olefins. US Patent 4025575.
Chen, D., Grlnvold, A., Moljord, K., Holmen, A., 2007. Methanol conversion to light olefins over SAPO-34: reaction network and deactivation kinetics. Ind. Eng. Chem. Res. 46, 4116–4123.
Fatourehchi, N., Sohrabi, M., Royaee, S.J., Mirarefin, S.M., 2011. Preparation of SAPO-34 catalyst and presentation of a kinetic model for methanol to olefin process (MTO). Chem. Eng. Res. Des. 89, 811–816.
Froment, G.F., Bischoff, K.B., De Wilde, J., 2010. Chemical Reactor Analysis and Design, third ed. John Wiley & Sons Inc., New York, NY, pp. 304–305.
Gayubo, A.G., Aguayo, A.T., Alonso, A., Bilbao, J., 2007. Kinetic modeling of the methanol-to-olefins process on a silicoaluminophosphate (SAPO-18) catalyst by considering deactivation and the formation of individual olefins. Ind. Eng. Chem. Res. 46, 1981–1989.
Gayubo, A.G., Aguayo, A.T., del Campo, A.E.S., Tarrio, A.M., Bilbao, J., 2000. Kinetic modeling of methanol transformation into olefins on a SAPO-34 catalyst. Ind. Eng. Chem. Res. 39, 292–300.
Gayubo, A.G., Aguayo, A.T., Moran, A.L., Olazar, M., Bilbao, J., 2002. Role of water in the kinetic modeling of catalyst deactivation in the MTG process. AIChE J. 48, 1561–1571.
Gayubo, A.G., Benito, P.L., Aguayo, A.T., Castilla, M., Bilbao, J., 1996. Kinetic model of the MTG process taking into account the catalyst deactivation. Reactor simulation. Chem. Eng. Sci. 51, 3001–3006.
Guisnet, M., 2002. Coke molecules trapped in the micropores of zeolites as active species in hydrocarbon transformations. J. Mol. Catal. A: Chem. 182, 367–382.
Haw, J.F., 2002. Zeolite acid strength and reaction mechanisms in catalysis. PCCP 4, 5431–5441.
Haw, J.F., Marcus, D.M., 2005. Well-defined (supra)molecular structures in zeolite methanol-to-olefin catalysis. Top. Catal. 34, 41–48.
Hereijgers, B.P.C., Bleken, F., Nilsen, M.H., Svelle, S., Lillerud, K.P., Bjorgen, M., Weckhuysen, B.M., Olsbye, U., 2009. Product shape selectivity dominates the methanol-to-olefins (MTO) reaction over H-SAPO-34 catalysts. J. Catal. 264, 77–87.
Jiang, G., Zhang, L., Zhao, Z., Zhou, X., Duan, A., Xu, C., Gao, J., 2008. Highly effective P-modified HZSM-5 catalyst for the cracking of C4 alkanes to produce light olefins. Appl. Catal., A: Gen. 340, 176–182.
Kaarsholm, M., Joensen, F., Nerlov, J., Cenni, R., Chaouki, J., Patience, G.S., 2007. Phosphorous modified ZSM-5: deactivation and product distribution for MTO. Chem. Eng. Sci. 62, 5527–5532.
Kaarsholm, M., Rafii, B., Joensen, F., Cenni, R., Chaouki, J., Patience, G.S., 2010. Kinetic modeling of methanol-to-olefin reaction over ZSM-5 in fluid bed. Ind. Eng. Chem. Res. 49, 29–38.
Keil, F.J., 1999. Methanol-to-hydrocarbons: process technology. Microporous Mesoporous Mater. 29, 49–66.
Keil, F.J., Hinderer, J., Garayhi, A.R., 1999. Diffusion and reaction in ZSM-5 and composite catalysts for the methanol-to-olefins process. Catal. Today 50, 637–650.
Liang, J., Li, H.Y., Zhao, S., Guo, W.G., Wang, R.H., Ying, M.L., 1990. Characteristics and performance of SAPO-34 catalyst for methanol-to-olefin conversion. Appl. Catal. 64, 31–40.
Marquardt, D.W., 1963. An algorithm for least-squares estimation of nonlinear parameters. J. Soc. Ind. Appl. Math. 11, 431–441.
Menges, M., Kraushaar-Czarnetzki, B., 2012. Kinetics of methanol to olefins over AlPO4-bound ZSM-5 extrudates in a two-stage unit with dimethyl ether pre-reactor. Microporous Mesoporous Mater. 164, 172–181.
Mihail, R., Straja, S., Maria, G., Musca, G., Pop, G., 1983. Kinetic model for methanol conversion to olefins. Ind. Eng. Chem. Process Des. Dev. 22, 532–538.
Mores, D., Stavitski, E., Kox, M.H., Kornatowski, J., Olsbye, U., Weckhuysen, B.M., 2008. Space-and time-resolved in-situ spectroscopy on the coke formation in molecular sieves: methanol-to-olefin conversion over H-ZSM-5 and H-SAPO-34. Chem. Eur. J. 14, 11320–11327.
Nayak, S.V., Joshi, S.L., Ranade, V.V., 2005. Modeling of vaporization and cracking of liquid oil injected in a gas–solid riser. Chem. Eng. Sci. 60, 6049–6066.
Park, T.Y., Froment, G.F., 2001a. Kinetic modeling of the methanol to olefins process. 1. Model formulation. Ind. Eng. Chem. Res. 40, 4172–4186.
Park, T.Y., Froment, G.F., 2001b. Kinetic modeling of the methanol to olefins process. 2. Experimental results, model discrimination, and parameter estimation. Ind. Eng. Chem. Res. 40, 4187–4196.
Qi, G.Z., Xie, Z.K., Yang, W.M., Zhong, S.Q., Liu, H.X., Zhang, C.F., Chen, Q.L., 2007. Behaviors of coke deposition on SAPO-34 catalyst during methanol conversion to light olefins. Fuel Process. Technol. 88, 437–441.
Schoenfelder, H., Hinderer, J., Werther, J., Keil, F.J., 1994. Methanol to olefins-prediction of the performance of a circulating fluidized-bed reactor on the basis of kinetic experiments in a fixed-bed reactor. Chem. Eng. Sci. 49, 5377–5390.
Sedran, U., Mahay, A., Delasa, H.I., 1990a. Modeling methanol conversion to hydrocarbons-alternative kinetic-models. Chem. Eng. J. 45, 33–42.
Sedran, U., Mahay, A., Delasa, H.I., 1990b. Modeling methanol conversion to hydrocarbons-revision and testing of a simple kinetic-model. Chem. Eng. Sci. 45, 1161–1165.
Stocker, M., 1999. Methanol-to-hydrocarbons: catalytic materials and their behavior. Microporous Mesoporous Mater. 29, 3–48.
Taheri Najafabadi, A., Fatemi, S., Sohrabi, M., Salmasi, M., 2012. Kinetic modeling and optimization of the operating condition of MTO process on SAPO-34 catalyst. J. Ind. Eng. Chem. 18, 29–37.
Tian, P., Wei, Y., Ye, M., Liu, Z., 2015. Methanol to olefins (MTO): from fundamentals to commercialization. ACS Catal. 5, 1922–1938.
Wei, Y., Yuan, C., Li, J., Xu, S., Zhou, Y., Chen, J., Wang, Q., Xu, L., Qi, Y., Zhang, Q., 2012. Coke formation and carbon atom economy of methanol-to-olefin reaction. ChemSusChem 5, 906–912.
Wu, X.C., Abraha, M.G., Anthony, R.G., 2004. Methanol conversion on SAPO-34: reaction condition for fixed-bed reactor. Appl. Catal., A: Gen. 260, 63–69.
Yang, G.J., Wei, Y.X., Xu, S.T., Chen, J.R., Li, J.Z., Liu, Z.M., Yu, J.H., Xu, R.R., 2013. Nanosize-enhanced lifetime of SAPO-34

catalysts in methanol-to-olefin reactions. J. Phys. Chem. C 117, 8214–8222.

Ying, L., Ye, M., Cheng, Y.W., Li, X., Liu, Z.M., 2013. A kinetic study of methanol to olefins (MTO) process in fluidized bed reactor. In: The 14th International Conference on Fluidization—From Fundamentals to Products, Noordwijkerhout, The Netherlands.

Zhao, Y.F., Li, H., Ye, M., Liu, Z.M., 2013. 3D numerical simulation of a large scale MTO fluidized bed reactor. Ind. Eng. Chem. Res. 52, 11354–11364.